WNT5A drives IL-6 dependent epithelial-to-mesenchymal transition via JAK/STAT pathway in keloid pathogenesis

Young In, Lee

Department of Medicine

The Graduate School, Yonsei University

WNT5A drives IL-6 dependent epithelial-to-mesenchymal transition via JAK/STAT pathway in keloid pathogenesis

Young In, Lee

Department of Medicine
The Graduate School, Yonsei University

WNT5A drives IL-6 dependent epithelial-to-mesenchymal transition via JAK/STAT pathway in keloid pathogenesis

Directed by Professor Ju Hee Lee

The Doctoral Dissertation submitted to the
Department of Medicine
the Graduate School of Yonsei University
in partial fulfillment of the requirements for the degree
of Doctor of Philosophy

Young In Lee

December 2020

This certifies that the Doctoral Dissertation
of Young In Lee is approved

Thesis Supervisor : Ju Hee Lee

Thesis Committee Chair : Kee Hyun Nam

Thesis Committee Member : Won Jai Lee

Thesis Committee Member : Jaewoo Kim

Thesis Committee Member : Mi Yeon Park

The Graduate School
Yonsei University

December 2020

ACKNOWLEDGEMENTS

I would first like to thank my thesis advisor Professor Ju Hee Lee for the continuous support of my study and research. Her guidance helped me as a lifetime mentor in all the time of research and practice as a dermatologist. Studying from Professor Lee's lab has been an invaluable experience of learning science and the greatest source of inspiration.

I sincerely appreciate my committee members, Professors Kee Hyun Nam, Won Jai Lee, Jaewoo Kim, and Mi Yeon Park who gave me constructive advices, innovative ideas and encouragements.

I would like to express my gratitude to the Professors in Department of Dermatology, Kwang Hoon Lee, Min-Geol Lee, Kee-Yang Chung, Sang Ho Oh, Chang Ook Park, Do Young Kim, Byung Ho Oh, Tae Gyun Kim, and Jihee Kim for their warm supports and making my unforgettable experiences during the graduate study.

I really appreciate the support of the lab members and colleagues, Soo Min Kim, Jemin Kim, Eun Bin Kim, and Seulgi Jang.

Finally, I must express my very profound gratitude to my parents and family for providing me with unfailing support and continuous encouragement throughout my years of study and through the process of researching and writing this thesis. This accomplishment would not have been possible without them. I wish to deeply thank my beloved husband, Yoon Bin Jung, for bringing enduring happiness and light into my life. I love you.

December 2020

Young In Lee

<TABLE OF CONTENTS>

III. RESULTS

LIST OF FIGURES

LIST OF TABLES

ABSTRACT

WNT5A drives IL-6 dependent epithelial-to-mesenchymal transition via JAK/STAT pathway in keloid pathogenesis

Young In Lee

Department of Medicine
The Graduate School, Yonsei University

(Directed by Professor Ju Hee Lee)

Keloid is a fibroproliferative disease caused by aberrant genetic activation of wound healing. The suggested causes of keloid pathogenesis include genetic predisposition, aberrant cellular responses to environmental mechanical strain, upregulation of inflammatory cytokines, and epithelial–mesenchymal transition (EMT). Here, we examined the molecular drivers contributing to keloid pathogenesis. We performed next-generation RNA sequencing on keloid and normal tissues to identify genes that contribute to keloid disease. Gene set enrichment analysis revealed upregulation of WNT5A gene expression, along with significant enrichment of genes related to EMT in keloid tissues. These results correlate with those of tissue analysis in which human keloid tissues showed increased WNT5A expression along with EMT markers. We established a preclinical model

of human keloid by injecting bleomycin intradermally for 3 weeks into C57/BL6 mice. Histological analysis revealed increased expression of WNT5A and EMT after skin fibrosis development from bleomycin injection. Our *in vitro* data using a human dermal fibroblast and primary keratinocyte co-culture system suggested that IL-6 secreted from WNT5A-activated fibroblasts induces keratinocytes to express EMT markers by activating the JAK/STAT signaling pathway. A better understanding of the keloid pathogenesis and role of WNT5A in EMT will promote the development of next-generation targeted treatments for keloid scars.

Key words: WNT5A, keloid, epithelial mesenchymal transition, fibrosis

WNT5A drives IL-6 dependent epithelial-to-mesenchymal transition via JAK/STAT pathway in keloid pathogenesis

Young In Lee

Department of Medicine
The Graduate School, Yonsei University

(Directed by Professor Ju Hee Lee)

I. INTRODUCTION

The ability of non-myeloid stem cells to differentiate into various other cell lineages has gained attention in the research field of cancer development. In epithelial-to-mesenchymal transition (EMT), epithelial cells acquire remarkable cell plasticity and differentiate into various types of mesenchymal cells[1]. Keloid scars are benign dermal fibroproliferative tumors that are unique to humans. These scars occur at areas of cutaneous injury and expand aggressively beyond the original margins of the scar[2]. Although keloids are non-malignant tumors that do not metastasize, their morphology and clinically aggressive behaviors resemble those of neoplastic tumors[3]. Recent studies on the pathogenesis of keloids revealed that their recurrence and invasiveness may primarily involve aberrant genetic activation of EMT during wound healing.

Malignant transformation of various types of carcinoma depends on EMT activation in neoplastic cells[4]. Upon activation of EMT, the cells acquire a

spindle-shaped morphology and highly express mesenchymal markers such as neural cadherin (N-cadherin), slug, vimentin, α-smooth muscle actin (α-SMA), and fibronectin[5]. During the pathologic transition of epithelial cells into mesenchymal cells, dissolution of cell-cell junctions, loss of apical-basal polarity, reorganization of the cytoskeletal architecture, and acquisition of the ability of degrade extracellular matrix proteins to enable invasive behavior can occur[6]. As keloid scars occur due to abnormal fibrosis that extends beyond the site of the original skin injury, EMT plays an important role in the development and aggravation of keloid scars[7,8].

Zhang et al. (2009) described a distinct population of self-renewing keloid-derived precursor cells expressing mesenchymal and embryonic stem cell markers driven by IL-6/IL-17 mediated inflammation. IL-6 is a pro-tumorigenic cytokine that is frequently elevated in keloid fibroblasts[9]. Interestingly, not only IL-6 but also its second messengers JAK/STAT3 are elevated in keloid fibroblasts, potentially contributing to tumorigenesis within the tumor microenvironment[10,11]. The IL-6/JAK/STAT3 pathway is also a key signaling pathway in the pathogenesis of EMT in other internal organ systems. Wang et al. (2018) showed that IL-6-dependent STAT3 activation positively regulated TGF-β1-induced EMT and invasion in hepatocellular carcinoma. A recent study of peritoneal fibrosis due to long-term peritoneal dialysis therapy concluded that IL-6 promoted EMT by activating the JAK/STAT3 pathway, causing fibrotic injury of the peritoneal membrane[12].

WNT5A is a secreted growth factor in the non-canonical Wnt family. In liver myofibroblasts, knockdown of WNT5A led to reduced production of IL-1β and IL-6 and the matrix proteins collagen type I and III, whereas WNT5A overexpression resulted in increased expression of these factors and enhanced cell proliferation[13]. Proteomics studies showed that WNT5A is significantly

upregulated in activated liver myofibroblasts[14]. In general, WNT5A expression during fibrosis is associated with myofibroblast proliferation and migration and the production of extracellular matrix proteins[15]. Igota et al. (2013) demonstrated that the mRNA and protein levels of WNT5A are increased in keloid fibroblasts compared to in normal fibroblasts. Thus, WNT5A may cause aberrant phenotypes in keloid fibroblasts; however, functional studies are needed to understand its pathophysiologic mechanisms.

Keloid scar is a chronic disfiguring condition that causes important physical and psychological impairments, but there is no single effective treatment targeting the fundamental mechanism of keloidogenesis. Upon injury, pathogenic keloid fibroblasts are thought to cause neighboring epidermal keratinocytes to produce keloid matrix features by expressing genes involved in EMT and upregulating the expression of inflammatory mediators such as IL-6. In this study, we examined the relationship between the Wnt signaling pathway and characteristic EMT phenomenon in keloids to identify a novel keloid biomarker and suggest potential treatment targets for suppressing pathogenic fibrosis of the skin.

II. MATERIAL AND METHODS

1. Patient samples and tissue handling

Keloid tissues from nine patients with active-stage keloids and undergoing surgical excision were harvested after obtaining informed consent according to the protocol approved by the Yonsei University College of Medicine Institutional Review Board (IRB No. 4-2017-0259). All samples were collected from patients who had developed abnormally growing

keloid scars for longer than 2 years. All experiments involving humans adhered to the Declaration of Helsinki. Tissue specimens from patients who underwent any type of treatment for keloid within the past three months were excluded. The fresh specimens were divided, immediately cut into 2-mm^3 pieces, and stored at -80°C after immersion in RNAlater solution. The remaining specimen were immersed in 10% neutral-buffered formalin and paraffin-embedded as formalin-fixed paraffin-embedded tissue samples.

2. RNA sequencing (RNA-seq)

A. Sample selection and RNA-seq

(1) Keloid scar tissue (n=9)

Total RNA was isolated from nine human keloid tissue samples using the RNeasy® Mini Kit (Qiagen, Hilden, Germany) following a standard extraction protocol. RNA integrity was evaluated with a Bioanalyzer 2100 (Agilent Technologies, Santa Clara, CA, USA). A library was prepared from 1 μg RNA per sample using the TruSeq RNA Library Prep Kit v2 (Illumina, San Diego, CA, USA). The quality of RNA sequencing paired-end reads was assessed with FastQC (Illumina). RNA-Seq libraries were constructed using a SureSelect^{XT} RNA-Seq Library Prep Kit (Agilent Technologies) and sequenced in 100-bp paired-end mode on a NextSeq550-platform. Sequencing was performed by the Genomics Core at Avison Biomedical Research Center, Yonsei University.

(2) Normal control tissue data from public data sources (N=11)

Two public data sets were assessed from the Sequence Read Archive (SRA)

database to establish a total of 11 normal control tissue data. Raw data (FASTQ files) from seven healthy skin biopsies sequenced on the NextSeq500-platform, generating 800 million total reads, were downloaded from the SRA database (accession number: SRP227263). Another raw dataset (FASTQ files) from four normal skin tissues sequenced on the Hiseq2000-platform were downloaded (accession number: ERP022968) The multiple normal tissue datasets were collected and used as control tissue data to reduce selection bias from using a single public dataset.

B. Total RNA-seq analysis and batch effect correction

The RNA-seq data were further analyzed from the Bioinformatics Collaboration Unit, Yonsei University College of Medicine. The newly generated in-house dataset for keloid tissues and two public control datasets were analyzed with an identical RNA-seq analysis pipeline. All FASTQ reads were trimmed for quality and adapter content using Trimmomatic v.0.32, and the data were aligned to the human reference genome known as Hg38 using HISAT2 v.2.1.0. To minimize mis-alignment by remaining rRNA reads, we additionally removed rRNA reads using RSeQC v.2.6.1. The data were then quantified as transcripts per million using StringTie v.2.0.6, and raw read counts retrieved using the Python script available from StringTie were used as input to the DESeq2 R package.

To overcome collinearity problem from utilizing multiple datasets, we modified *scBatch* method[16], one of the assumption-free batch effect correction algorithms, to correct the quntile distribution from the distinct batch blocks in the sample distance matrix. Sample distances were measured using the correlation with the expression matrix of the housekeeping genes, which characteristically maintained constant expression levels in all biologic conditions. To adjust for batch effects, 98 housekeeping genes compiled in a previous study were utilized [17].

C. Differential Expression (DE) analysis on DESeq2

The genes that differed significantly between the two groups, the keloid scar and normal tissues, were identified with DESeq2 v.1.26.0. DESeq2 R package, one of the count-based methods for analysis, received count matrix corrected for the batch effect as the input. The genes with non-zero expression values in at least 3 samples from each dataset of 9 keloids and 11 controls were extracted. Only those genes that exhibited logarithmic changes (base 2) in expression > 0.5-fold, and the adjusted p-values using the Benjamini–Hochberg procedure lower than 0.01 (p.adj < 0.01) were considered as differentially expression genes (DEG). Finally, 1,939 up-regulated genes and 1,610 down-regulated genes were selected as DEGs.

3. Cell culture and transfection

Adult human primary epidermal keratinocytes (HEKa, ATCC, Manassas, VA, USA, PCS-200-011) were prepared and maintained in a tissue incubator. Experiments were conducted with HEKs at passages 2–4. Normal HDFs and KFs were purchased from ATCC. Cells were cultured in DMEM (Gibco, Grand Island, NY, USA) containing 10% heat-inactivated FBS, actinomycin, penicillin (30 U/mL), and streptomycin (300 μg/mL). The culture medium was replaced every 2–3 days. A total of 5×10^5 HDFs or KFs were treated with WNT5A (250 ng/mL; 645-WN-010, R&D Systems, Minneapolis, MN, USA) for the times indicated, whereas 5×10^5 HEKs were treated with recombinant human IL-6 (50 ng/mL; 206-IL-010, R&D Systems) and cultured in “serum-free” media overnight before treatment. siRNA targeting WNT5A (siWNT5A) was applied to silence WNT5A. Cells were transfected either with control siRNA (D-001810-10-05; Dharmacon, Lafayette, CO, USA) and siWNT5A (L-003939-00-0005; Dharmacon, Lafayette, CO, USA) using Lipofectamine (Invitrogen, Carlsbad, CA, USA) according to the manufacturer’s instructions.

4. Establishment of the co-culture system of HDFs and HEKs

HEKs (5×10^5) were seeded into the lower chamber and HDFs (5×10^5) into the upper chamber of a 6.5-mm diameter transwell chamber separated by a 0.4-μm pore-size membrane (Corning, Inc., Corning, NY, USA) and cultured in DMEM containing 10% heat-inactivated FBS, actinomycin, penicillin (30 U/mL), and streptomycin (300 μg/mL). Co-cultures were incubated with or without WNT5A (250 ng/mL) for the times indicated at 37°C and 5% CO_2. To investigate the effect of IL-6 neutralization on the co-culture system, human neutralizing IL-6 antibodies (10 μg/mL, MAB2061-SP; R&D Systems) were added to the chamber. At each sampling time, conditioned media from the upper chamber were collected. The supernatants of each stimulation experiment with or without WNT5A were collected and stored at -80°C. HEKs from the lower chamber were washed three times with PBS and collected for further experiments. The results were obtained from 5 independent experiments.

5. Preparation of animals and bleomycin-induced skin fibrosis model

Specific-pathogen-free 6-week-old female C57/BL6 mice weighing 20–25 g were purchased from the ORIENT BIO Animal Center (Seongnam-si, Korea). Mice were reared in a temperature-controlled room at 24 ± 20°C and 55 ± 15% humidity with a 12-h light and dark cycle. Before the experiment, mice underwent a 1-week acclimation period. Seven- to 12-week-old mice were used in all experiments. Injection of 100 μL of 1 mg/mL bleomycin sulfate (S1214; Selleckchem, Houston, TX, USA) was performed at 1-cm^2 shaved back skins of the mice 5 times per week for 3 weeks as previously described [18]. All experiments were conducted in accordance with the Guide for the Care and Use of Laboratory Animals provided by the Animal Laboratory Ethics Committee of the Department

of Laboratory Animal Medicine, Medical Research Center, Yonsei University College of Medicine.

6. Immunohistochemistry

The tissue samples were cut into 4-μm-thick slices for immunohistochemistry analysis, deparaffinzed with xylene, and hydrated using graded ethanol. The samples were stained with H&E and a Masson's Trichrome (MT) Stain Kit (ab150686; Abcam, Cambridge, UK) according to the manufacturer instructions. Antigen retrieval was performed using an antigen retrieval solution (Dako, Carpinteria, CA, USA), and a rabbit polyclonal IgG primary antibody to WNT5A (Abcam, 1:100) and mouse monoclonal IgG antibody to vimentin (Abcam, 1:100) were used. The REAL EnVision HRP Rabbit/Mouse Detection System (Dako) secondary antibody were used. Samples were visualized using the chromogen 3,3′-diaminobenzidine, and counter-staining was performed using hematoxylin. Immunohistochemistry stained keloid sections were semi-quantitatively analyzed using ImageJ software (National Institutes of Health, Bethesda, MD, USA). All analyses were performed on images (original magnification, 100x) generated from 3 tissue sections from each study group, and the average data were statistically analyzed.

7. Immunofluoresence

Double immunofluorescence stainings of WNT5A with cytokeratin 14 (Abcam, 1:100), PECAM-1 (Santa Cruz Biotechnology, 1:100), α-SMA (Abcam, 1:100), CD34 (Santa Cruz Biotechnology, 1:100) were performed to determine cell localization and differential expression of WNT5A in keloid and normal tissues. After 24 h of co-incubation, sections were washed with PBS and incubated

with secondary antibodies for 1 h. Sealed with 50% glycerol, sections were observed and photographed under fluorescence microscope. All fluorescence images were observed under Zeiss Confocal LSM 700 microscope (Zeiss, Oberkochen, Germany).

8. RNA isolation and Real-time PCR analysis

Total RNA was extracted from the cells using RNAiso plus reagent (#9109, Takara Biotechnology Co., Ltd., China) and purified using the RNeasy Plus Mini Kit (Qiagen) according to manufacturer instructions. RNA was quantified using NanoDrop 2000 spectrophotometer (NanoDrop Tech., Wilmington, DE, USA). RNA was reverse transcribed to cDNA using the RNA to cDNA EcoDry Premix Kit (Takara Bio, Kusatsu, Shiga Prefecture, Japan). Quantitative reverse transcription PCR (qRT-PCR) was performed using the QuantStudio 3 Real-Time PCR System (Applied Biosystems, Foster City, CA, USA) in 20-μL reactions containing SYBR Green Master Mix (Promega, Madison, WI, USA) and specific primer pairs (Macrogen, Seoul, Korea). Primer sequences are listed in Table 1. Cycling conditions were as follows: 95°C for 10 min, followed by 40 cycles of 95°C for 15 s, 60°C for 20 s, and 72°C for 30 s. mRNA levels were calculated by the relative quantification (ΔΔCt) method, with expression levels normalized to that of the housekeeping gene, glyceraldehyde 3-phosphate dehydrogenase (GAPDH).

Table 1. Primer lists

Target gene	Primer sequences (5'- 3')
WNT5A	Forward: TACGAGAGTGCTCGCATCCTCA Reverse: TGTCTTCAGGCTACATGAGCCG
VIM (vimentin)	Forward: AGGCAAAGCAGGAGTCCACTGA Reverse: ATCTGGCGTTCCAGGGACTCAT
SNAI2 (slug)	Forward: ATCTGCGGCAAGGCGTTTTCCA Reverse: GAGCCCTCAGATTTGACCTGTC
CDH2 (N-cad)	Forward: CCTCCAGAGTTTACTGCCATGAC Reverse: GTAGGATCTCCGCCACTGATTC
CDH1 (E-cad)	Forward: GCCTCCTGAAAAGAGAGTGGAAG Reverse: TGGCAGTGTCTCTCCAAATCCG
COL1A1	Forward: GATTCCCTGGACCTAAAGGTGC Reverse: AGCCTCTCCATCTTTGCCAGCA
α-SMA	Forward: GCACCCCTGAACCCCAAGGC Reverse: GCACGATGCCAGTTGTGCCT
IL-6	Forward: AGACAGCCACTCACCTCTTCAG Reverse: TTCTGCCAGTGCCTCTTTGCTG
GAPDH	Forward: GTCTCCTCTGACTTCAACAGCG Reverse: ACCACCCTGTTGCTGTAGCCAA

9. ELISA

A pre-coated Human ELISA kit (IL-6, PeproTech, Rocky Hill, NJ, USA) was used to analyze cytokine secretion in the culture medium. IL-6 levels in the supernatants of fibroblasts and keratinocytes were quantified by ELISA according to the manufacturer instructions. Multiple samples were evaluated in each experiment; experiments were repeated three times independently.

10. Proteome profiler human cytokine array

The cytokine profile assay was performed using the Proteome Profiler Human Cytokine Array (#ARY0005B; R&D Systems) following the manufacturer's instructions. After incubating 5×10^5 HDFs and 5×10^5 KFs for 24 h, 1 mL of supernatant from each sample was added to 0.5 mL of array buffer 4 in separate tubes, followed by adding 15 μL of reconstituted Human Cytokine Array Detection Antibody Cocktail. The sample/antibody mixtures were cultured at room temperature for 1 h and then transferred to a 4-well multi-dish with antibody-coated membranes for overnight culture. Streptavidin-HRP was diluted in array buffer 5 and incubated with the array membrane for 30 min. Chemi Reagent Mix (1 mL) was added to each membrane for 1 min. The membranes were detected by exposure to X-ray film for 10 min.

11. Western blot analysis

A. Western blotting analysis

Cells were harvested and lysed in RIPA lysis buffer (Biosesang, Seongnam, Korea) containing protease inhibitor (PPI 1015, Quartett, Berlin, Germany), and protein concentrations were determined using a BCA protein assay (Sigma-Aldrich, St. Louis, MO, USA). Protein (20 μg) was fractionated by SDS-PAGE and transferred to nitrocellulose membranes. Membranes were immunoblotted with specific primary antibodies overnight at 37°C followed by secondary antibodies conjugated to HRP. Immunoblots were developed with ECL reagent (Ab Frontier, Seoul, Korea) and monitored with a luminescence image analyzer (LAS-4000 Mini, Fujifilm Life Sciences Tokyo, Japan). The optical densities of the bands on the developed film were analyzed using ImageJ software. Protein

levels were normalized to that of GAPDH or to the ratio of phosphorylated and total isoforms. Relative quantitation is expressed as the fold-induction compared to control conditions.

B. Antibodies and reagents

WNT5A (ab229200, ab235966), vimentin (ab8978), α-SMA (ab7817), COL1A (ab260043), cytokeratin14 (ab7800), STAT3 (ab68153), and *p*-STAT3(ab76315) were purchased from Abcam. Slug (C79G7), N-cadherin (#13116), E-cadherin (#14472), and GAPDH (#2118) were purchased from Cell Signaling Technology (Danvers, MA, USA). Beta-actin (sc-47778), CD34 (sc-7324), and PECAM-1(sc-1506) were purchased from Santa Cruz Biotechnology (Dallas, TX, USA). All antibodies were stored at -20°C.

12. Statistical analysis

Data are shown as the mean ± standard error of the mean and were analyzed using Mann-Whitney U test, with $p < 0.05$ considered as statistically significant. SPSS version 23.0 (SPSS, Inc., Chicago, IL, USA) was used for all statistical analyses (*$p < 0.05$, **$p < 0.01$, ***$p < 0.005$).

III. RESULTS

1. RNA sequencing analysis reveals differential expression of WNT5A and EMT markers in keloid and normal tissues

To explore specific features of human keloid compared to normal tissue, we performed RNA sequencing to comprehensively define the transcriptomic changes in keloid pathogenesis. We utilized in-house generated keloid RNA-seq data and two independent public datasets as the normal control data. After removing batch effects as previously described, principal component analysis of all genes showed that the two independent public datasets generated from different batches were combined into one group. Moreover, keloid and normal samples showed significant dispersion, demonstrating meaningful biological differences (Fig. 1A-B).

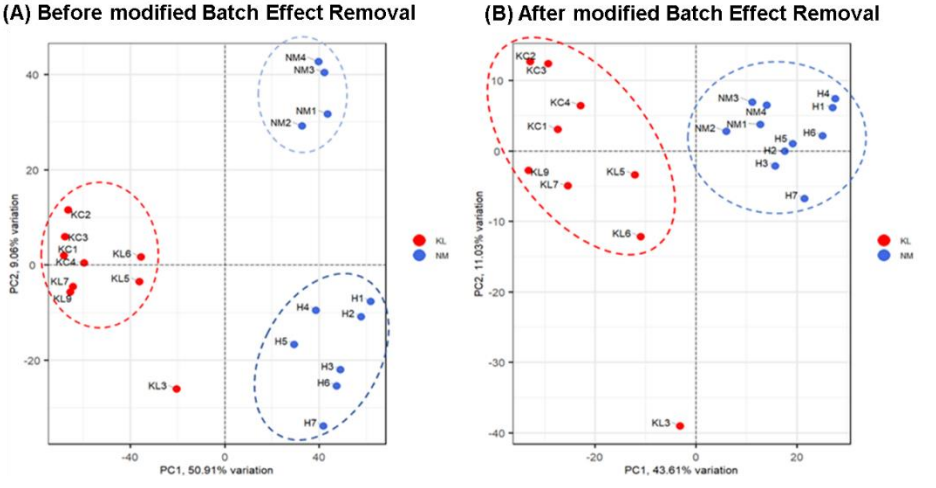

Figure 1. PCA plot analysis. PCA plot for all genes after removing batch effect (A) before modified batch effect removal and (B) after modified batch effect removal.

Genes differing significantly between the keloid scars and normal tissues were identified using DESeq2 v.1.26.0. Only genes exhibiting greater than 0.5-fold logarithmic changes in expression and with p-values adjusted using the Benjamini–Hochberg procedure lower than 0.01 ($p.adj < 0.01$) were considered as differentially expressed (DEG). As the result, 1,939 and 1,610 up- and down-regulated genes, respectively, were selected as the DEGs (Fig. 2). One-way hierarchical clustering showing systemic variations in the samples revealed that the DEGs could be selectively utilized to distinguish keloid samples from normal samples (Fig. 2).

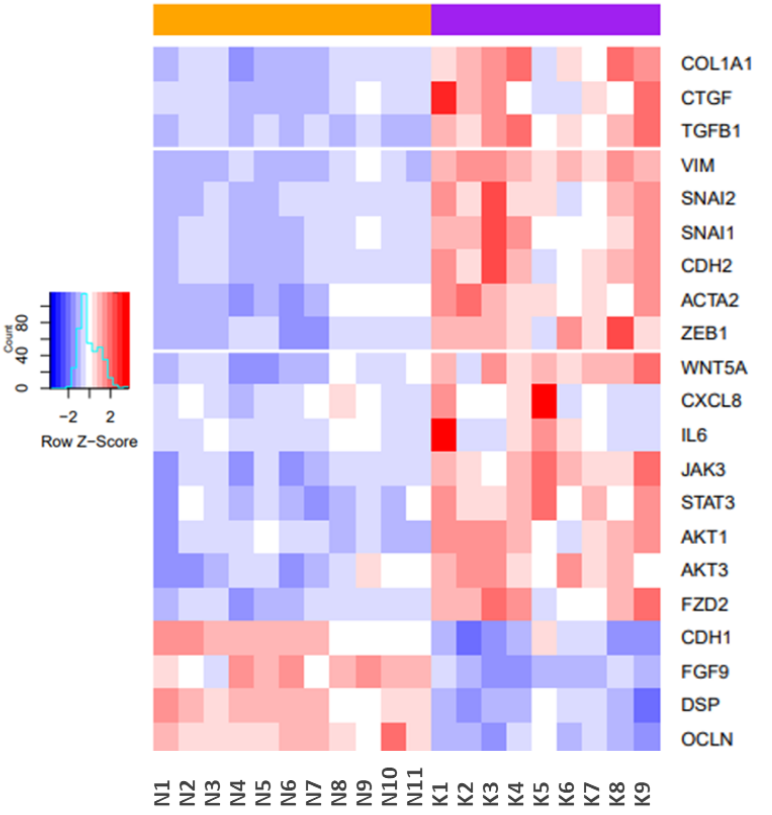

Figure 2. Heatmap for the DEGs showing upregulation of WNT5A and genetic markers of EMT in keloid samples.

Among various candidates, transcript level of WNT5A was significantly upregulated in the keloid samples by the log2FoldChange of 1.72 before the modified batch effect removal (adjusted p = 7.6 x 10^{-10}), and 0.637 after the removing the batch effect (adjusted p = 2.7 x 10^{-7}). The pathway analysis using gene set enrichment analysis (GSEA; v2.07, Broad Institute, Cambridge, MA) were performed and the top 10 pathways with the highest normalized enrichment scores (NES) were visualized in GSEA table (Fig. 3A). Notably, HALLMARK Epithelial Mesenchymal Transition pathway showed the highest NES containing the most significantly enriched gene sets (NES=3.06, p=1.8 x 10^{-4}, Fig. 3B), emphasizing upregulation of EMT related genes in keloid samples. Among related signaling pathways in keloid pathogenesis, HALLMARK IL6/JAK/STAT pathway revealed significant NES (NES=1.98, p = 0.002, Fig 3C).

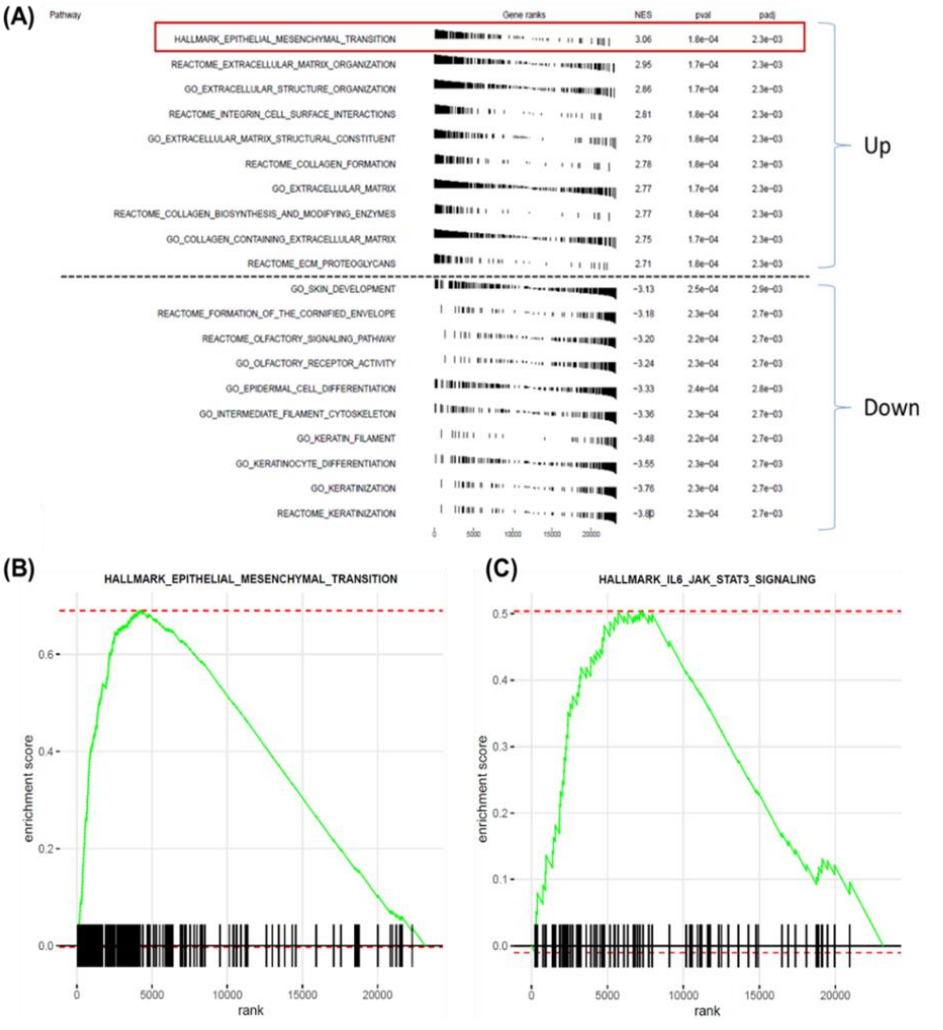

Figure 3. GSEA analysis. (A) Plot GSEA table showing top 10 NES reveals upregulation of epithelial to mesenchymal transition pathway in keloid samples. (B) Hallmark Epithelial Mesenchymal Transition pathway shows most significantly enriched genes set upregulated in keloid samples. (C) Hallmark IL6/JAK/STAT pathway shows a significantly upregulated NES in the keloid samples compared to the normal samples.

2. Human keloid tissue shows increased dermal thickness and abnormally thickened collagen bundles compared to normal tissues

H&E and Masson's trichrome staining of the human keloid tissues showed excessive and abnormally thick bundles of collagen fibers, and increased dermal thickness compared to the normal tissues (Fig. 4A-D). Additionally, mRNA expression levels of collagen 1A was significantly upregulated in keloid tissues compared to the normal tissues (Fig. 4E).

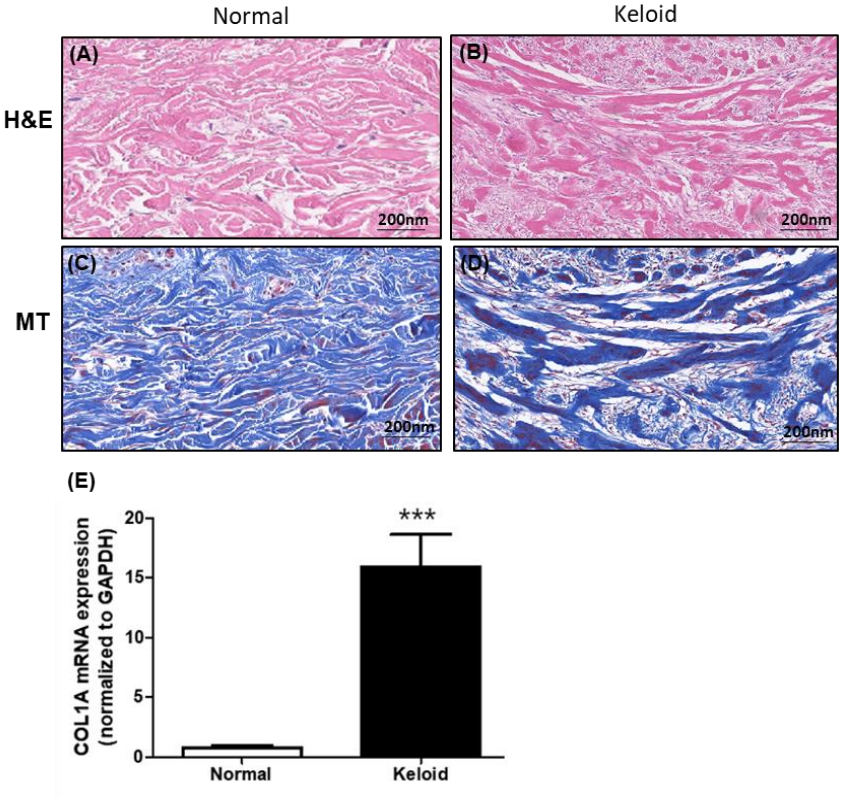

Figure 4. Immunohistochemistry for normal and keloid human tissues. (A-B) Human keloid shows abnormally thickened collagen bundles in H&E and (C-D) Masson's trichrome staining. (E) Collagen 1A mRNA expression shows higher expression in keloids (***$p < 0.005$). Scale bars indicate 200 μm.

3. Human keloid shows increased expressions of vimentin and α-SMA

The IHC staining of one of the representative EMT marker, vimentin, showed significantly higher expression in keloid tissues compared to normal tissues (Fig. 5A-B). The mRNA expression level of α-SMA, another key EMT marker, confirmed the elevated levels of EMT markers in keloid tissues (Fig. 5C). The semi-quantitative analysis of vimentin in keloid tissue was significantly higher in keloids than in normal tissues (Fig. 5D).

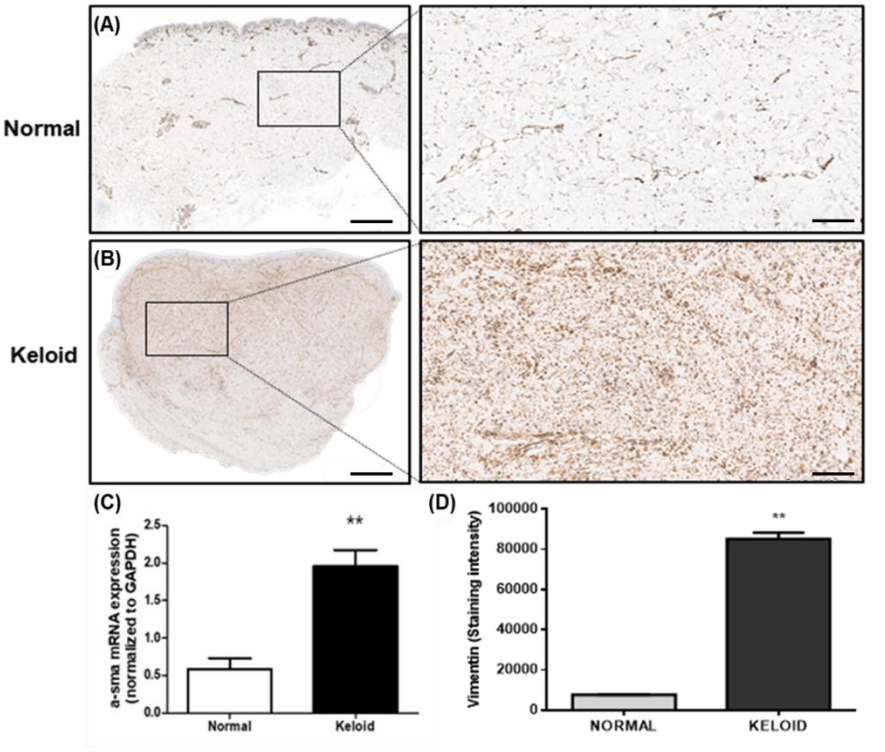

Figure 5. Keloid shows increased expressions of EMT markers. IHC staining shows increased vimentin expression in keloid tissue (A-B). The mRNA expression of α-SMA is higher in keloid tissue (C, $^{**}p < 0.01$). Percentage of positive area of vimentin is significantly higher in keloid (D, $^{**}p < 0.01$). Scale bars indicate 2mm on LPF, 300μm on HPF.

4. N-cadherin expression increase while E-cadherin expression decrease in human keloid tissues, confirming EMT phenomenon in keloid pathogenesis

To further verify the EMT phenomenon from human tissues, we performed immunohisotochemical staining for additional EMT markers, N-cadherin and E-cadherin. It is known that the upregulation of N-cadherin followed by the downregulation of E-cadherin is the hallmark of EMT[19]. Our study revealed that the expression of N-cadherin increased compared to the normal tissue (Fig. A-B). On the other hand, the expression of E-cadherin decreased in keloids compared to normal skin (Fig. 6A-B). These findings suggest that the EMT phenomenon occurred in keloid tissues.

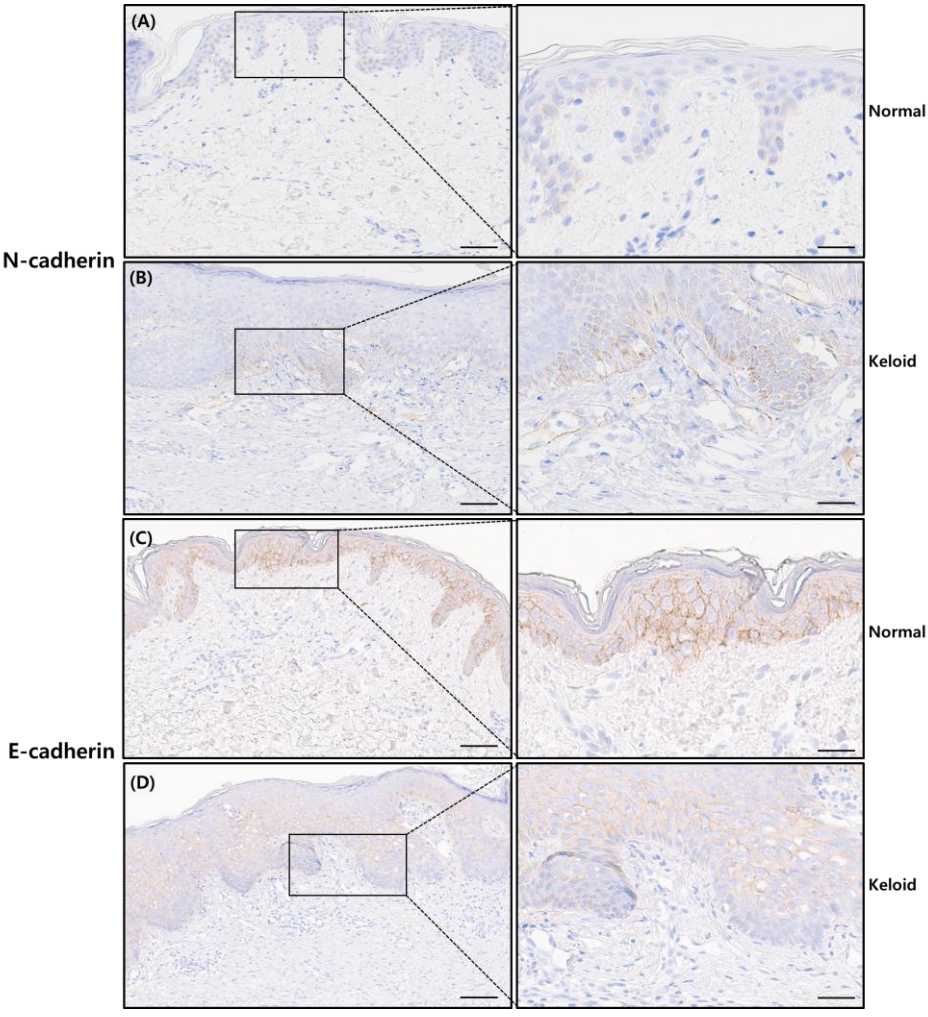

Figure 6. Keloid shows increased expressions of N-cadherin and decreased expression of E-cadherin. IHC staining shows increased N-cadherin expression in keloid tissue (A-B). The E-cadherin expression is decreased in keloid tissue (C-D*).* Scale bars indicate 100μm on LPF, 50μm on HPF.

5. Immunohistochemistry of human keloid tissue compared to normal tissue shows increased expression of WNT5A in keloid tissue

WNT5A showed increased expression in keloid tissues compared to the normal tissues, especially in the dermal regions (Fig. 7A-B). The semi-quantitative analysis from the immunohistochemical study confirmed that the expression of WNT5A was higher in keloid tissue (Fig. 7C). The subsequent qRT-PCR analysis on WNT5A also showed an increased level of WNT5A on keloid tissue compared to the normal control tissues (Fig. 7D).

To determine which cell type in the dermis expressed high levels of WNT5A in keloid tissues, we performed double immunofluorescence staining of WNT5A with markers for fibroblasts, endothelial cells, mast cells, and macrophages. As the result, the co-expression of WNT5A with fibroblasts was most significantly upregulated in keloid tissues compared to in normal tissues (Fig. 7E). Hence, higher expression of WNT5A in keloids may have resulted from the increased expression of WNT5A in keloid fibroblasts compared to in normal fibroblasts.

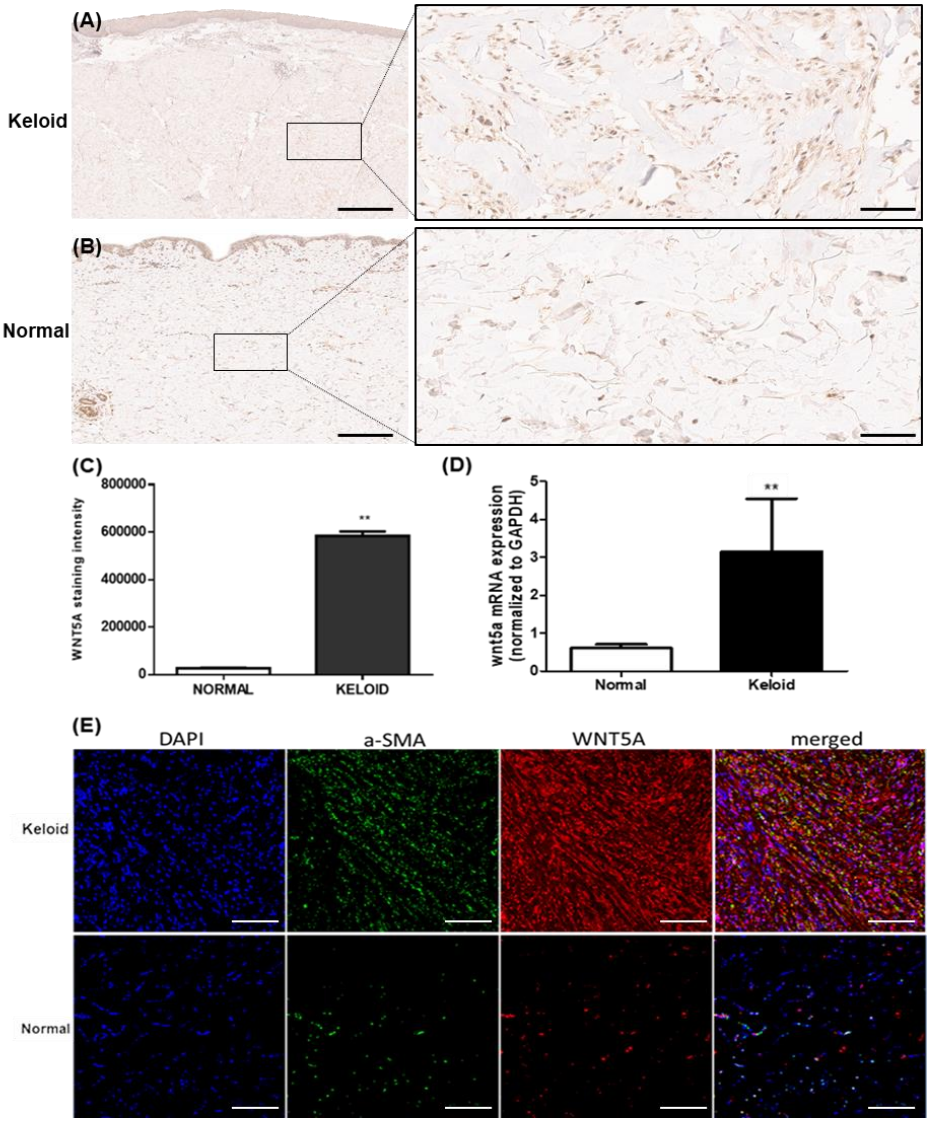

Figure 7. Keloid expresses higher level of WNT5A compared to normal tissue. Immunohistochemical staining of keloid tissue showed higher expression of WNT5A (A-C). qRT-PCR analysis showed higher WNT5A mRNA expression level in keloid tissue (C-D, $^{**}p < 0.01$). The double-immunofluorescence staining analysis shows higher expression of WNT5A in keloid tissue compared to normal tissue (E). Scale bars indicate 200μm on LPF, 50μm on HPF.

6. Keloid fibroblasts express higher levels of WNT5A and produce increased levels of pro-inflammatory cytokines compared to normal fibroblasts

To investigate the effect of WNT5A, we performed a human cytokine profile array to compare cytokine secretion between KFs and HDFs. Interestingly, KFs produced elevated levels of multiple pro-inflammatory cytokines, such as CCL2, IL-8, and IL-6, and CXCL-1, compared to HDFs, suggesting a role for WNT5A in activating secretion of these cytokines in fibroblasts (Fig. 8).

Additional immunofluorescence analysis showed significantly higher expression of WNT5A in keloid fibroblasts (KFs) compared to in human dermal fibroblasts (HDFs) (Fig. 9A). qRT-PCR confirmed higher expression of WNT5A and EMT markers (vimentin, N-cadherin, α-SMA) and decreased expression of E-cadherin from KFs compared to in HDFs (Fig. 9B-F). These results are consistent with previous immunohistochemical staining and qRT-PCR results, and suggest that elevated level of WNT5A in KFs drives increased secretions of pro-inflammatory cytokines from keloids.

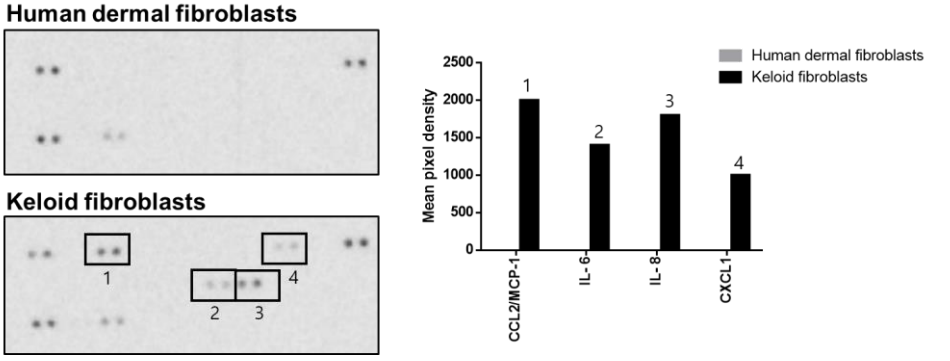

Figure 8. Human cytokine profile array. The cytokine array revealed increased secretion of pro-inflammatory cytokines from keloid fibroblasts compared to normal fibroblasts.

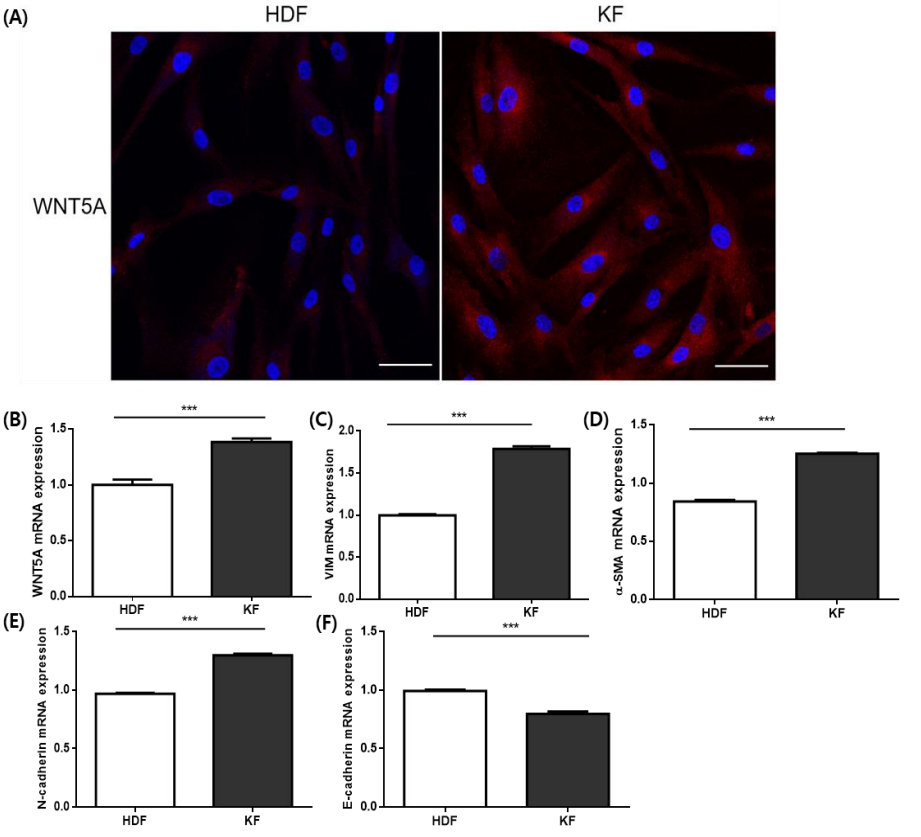

Figure 9. Keloid fibroblasts expressed higher level of WNT5A compared to HDFs. Immunohistochemical staining of WNT5A shows higher expression from KFs compared to HDFs (A). The mRNA expressions of WNT5A (B), VIM (C), a-SMA (D), N-cadherin (E) showed significantly higher expression in KFs compared to HDFs. E-cadherin (F) showed significantly lower expression in KFs compared to HDFs. All mRNA expression levels were normalized to GAPDH. Scale bars indicate 20μm. ***$p < 0.005$.

7. The daily intradermal injection of bleomycin on C57BL/6 mice induce sufficient dermal fibrosis at week 3

The animal model of skin fibrosis was established by daily injection of 100 μL of 1 mg/mL bleomycin sulfate intradermally into 1 × 1-cm^2-sized areas on the shaved back skins of C57BL/6 mice for 3 weeks (Fig. 10A-B). Both H&E and MT staining showed sufficient formation of dermal fibrosis at week 3, with an abnormally thick connective tissue layer and increased blue-stained materials, indicating collagen bundles (Fig. 10C). The dermal thickness after 3-week bleomycin injection was also significantly increased compared to in normal and 3-week PBS-injected control skin (Fig. 10D, $^{**}p < 0.01$). Semi-quantitative analysis showed a significant increase in collagen after 3 weeks of bleomycin injection compared to the control (Fig. 10E, $^{***}p < 0.005$).

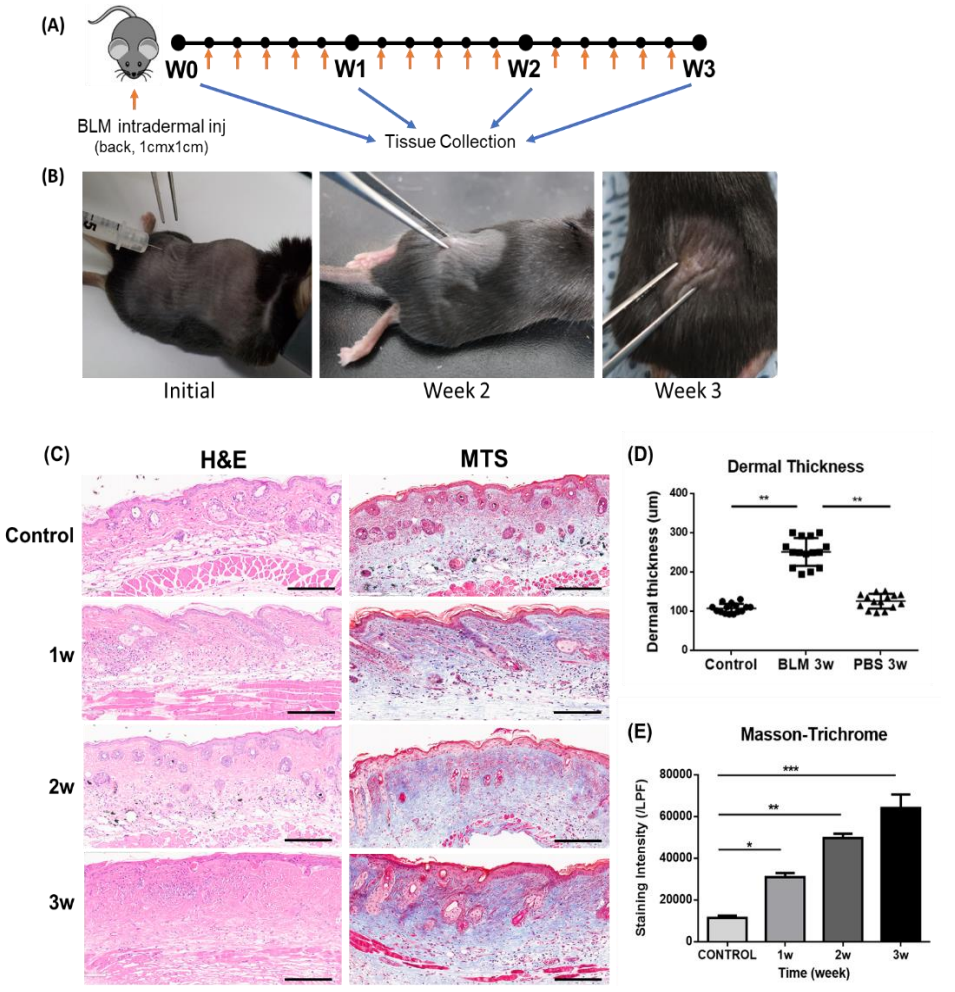

Figure 10. The bleomycin-induced fibrosis model in C57/BL6 mice. Daily injection of intradermal bleomycin established significant accumulation of collagen in the dermis after 3 weeks (A-C). H&E staining showed significantly increased dermal thickness after injection of bleomycin, compared to the normal and PBS-injection control skins (D, $^{**}p<0.01$). The semi-quantitative analysis from MT staining showed a significant increase in collagen after the bleomycin injection (E, $^{***}p<0.005$). Scale bar indicates 200μm from H&E and MT staining.

8. Expression level EMT marker is elevated in the bleomycin-induced dermal fibrosis model of C57BL/6 mice tissue

Immunohistochemistry analysis of the bleomycin-induced dermal fibrosis animal model showed that vimentin expression was significantly increased at week 3 compared to in the control (Fig. 11A). Semi-quantitative analysis of stained tissues confirmed the increased vimentin expression in bleomycin-injected tissues at week 3 (Fig. 11B, $p < 0.005$). qRT-PCR of the tissues also showed increased mRNA expression of vimentin (Fig. 11C, $p < 0.005$). This result confirmed that bleomycin-induced dermal fibrosis mice expressed increased EMT markers, similar to in human keloid tissues. Hence, this animal model can be used to investigate the pathogenesis of EMT in keloids.

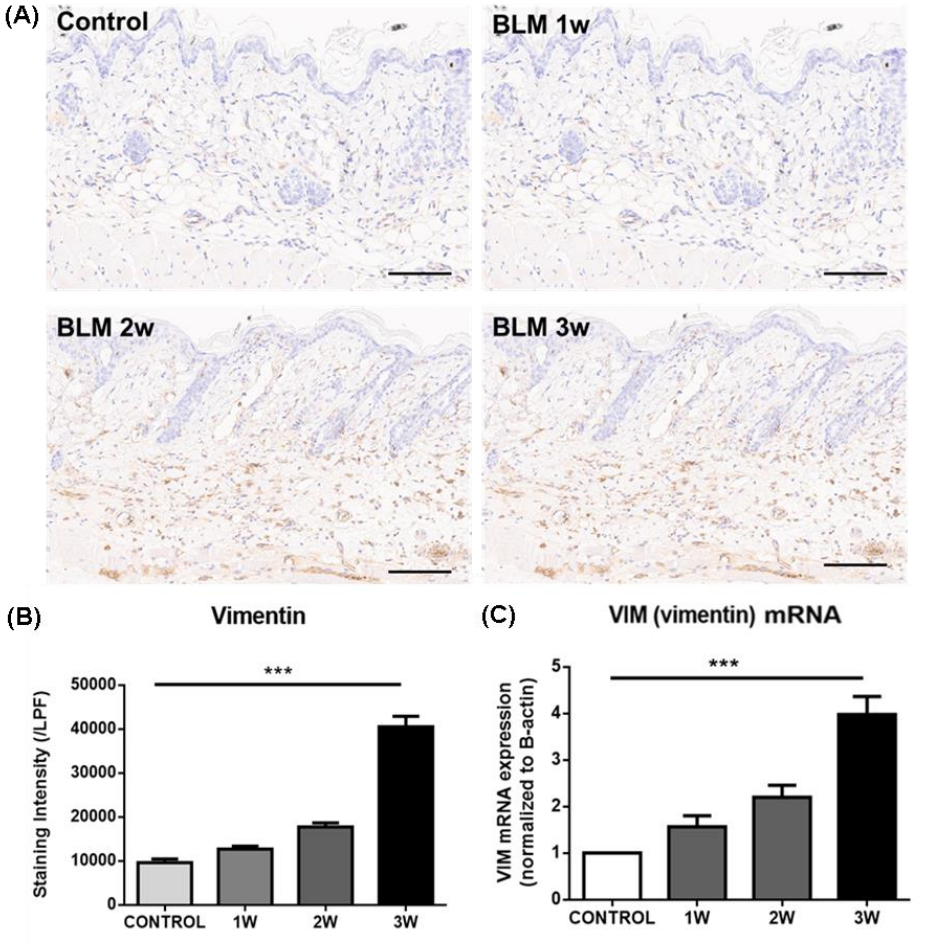

Figure 11. Increased expression of vimentin in the bleomycin-induced dermal fibrosis animal model. The immunohistochemistry revealed increased expression of vimentin throughout the dermis after intradermal bleomycin injection in mice (A). The semi-quantitative analysis showed increased vimentin after bleomycin injection at week 3 compared to the control (B). The tissue PCR showed increased VIM mRNA expression after intradermal bleomycin in injection (C). Scale bar indicates 100μm from the immunohistochemical staining.

9. The expression of WNT5A elevated in the bleomycin-induced dermal fibrosis model of C57BL/6 mice tissue

The expression of WNT5A, similar to vimentin, was increased after bleomycin injection at week 3 throughout the dermis (Fig. 12A). The semi-quantitative analysis of WNT5A from the tissue immunohistochemical staining also revealed increased WNT5A expression on bleomycin-induced dermal fibrosis tissue (Fig. 12B, $p < 0.005$). The mRNA expression level of WNT5A was also increased after the 3-week bleomycin injection compared to the control tissue (Fig. 12C, $p < 0.005$). These findings indicate that fibrotic tissue induced by bleomycin-injection in animal skin result in increased expression of WNT5A, similar to the human keloid tissues.

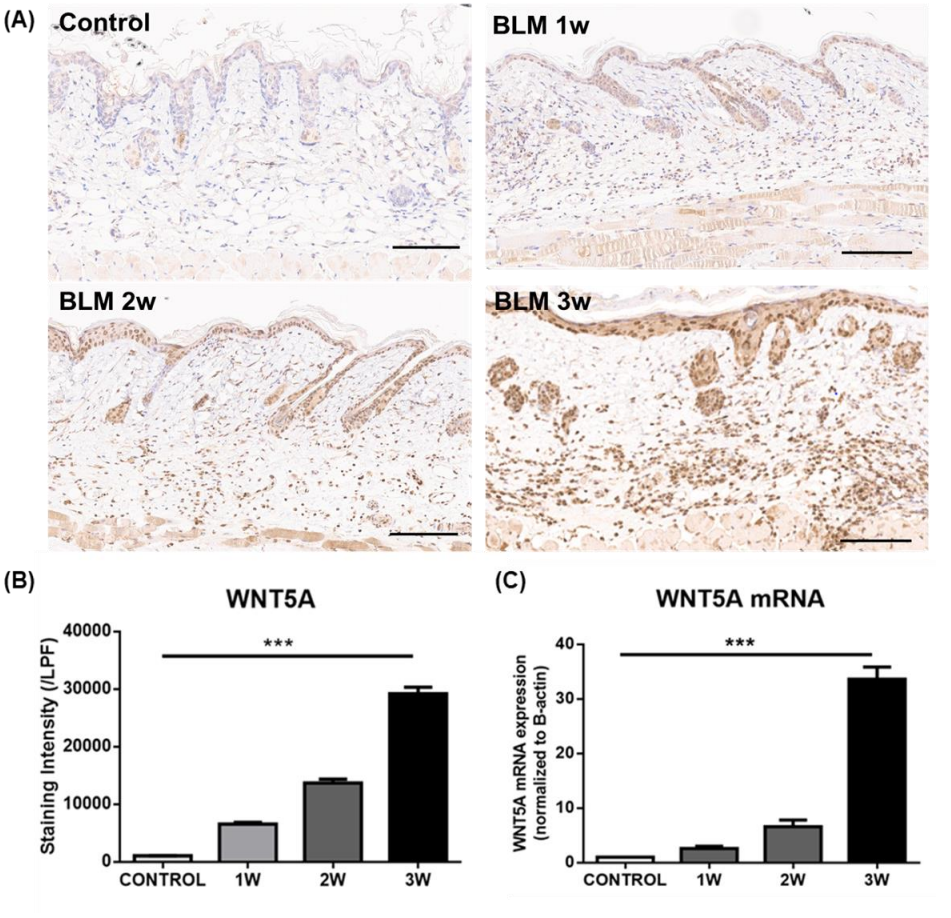

Figure 12. Increased expression of WNT5A in the bleomycin-induced dermal fibrosis animal model. The immunohistochemistry revealed increased expression of WTN5A throughout the dermis after intradermal bleomycin injection in mice (A). The semi-quantitative analysis showed increased WNT5A after bleomycin injection at week 3 compared to the control (B). The tissue PCR showed increased WTN5A mRNA expression after intradermal bleomycin in injection (C). Scale bar indicates 100μm from the immunohistochemical staining.

10. Human epidermal keratinocytes express higher levels of EMT markers when co-cultured with WNT5A-treated HDFs

To investigate the pathogenesis of keloid scar formation *in vitro*, a co-culture system between human epidermal keratinocytes (HEKs) and HDFs utilizing a transwell insert was designed. 5×10^5 HEKs were seeded into the lower chamber, whereas 5×10^5 HDFs were seeded into the upper chamber. In the control group, the same number of HEKs was seeded into the lower chamber without the upper layer seeding of HDFs (Fig. 13A). The HEK group and co-culture group of HEKs and HDFs were then divided into two groups, with or without the treatment with 250 ng/mL of WNT5A. HEKs co-cultured with HDFs expressed significantly higher levels of EMT makers (vimentin, slug, N-cadherin) when treated with WNT5A, whereas HEKs cultured alone did not (Figure 13B-D, $*p < 0.05$, $**p < 0.01$, repeated measures ANOVA). Based on these findings, it was hypothesized that WNT5A aberrantly activated HDFs, and chemical mediators secreted by the activated HDFs affected co-cultured HEKs and resulted in EMT.

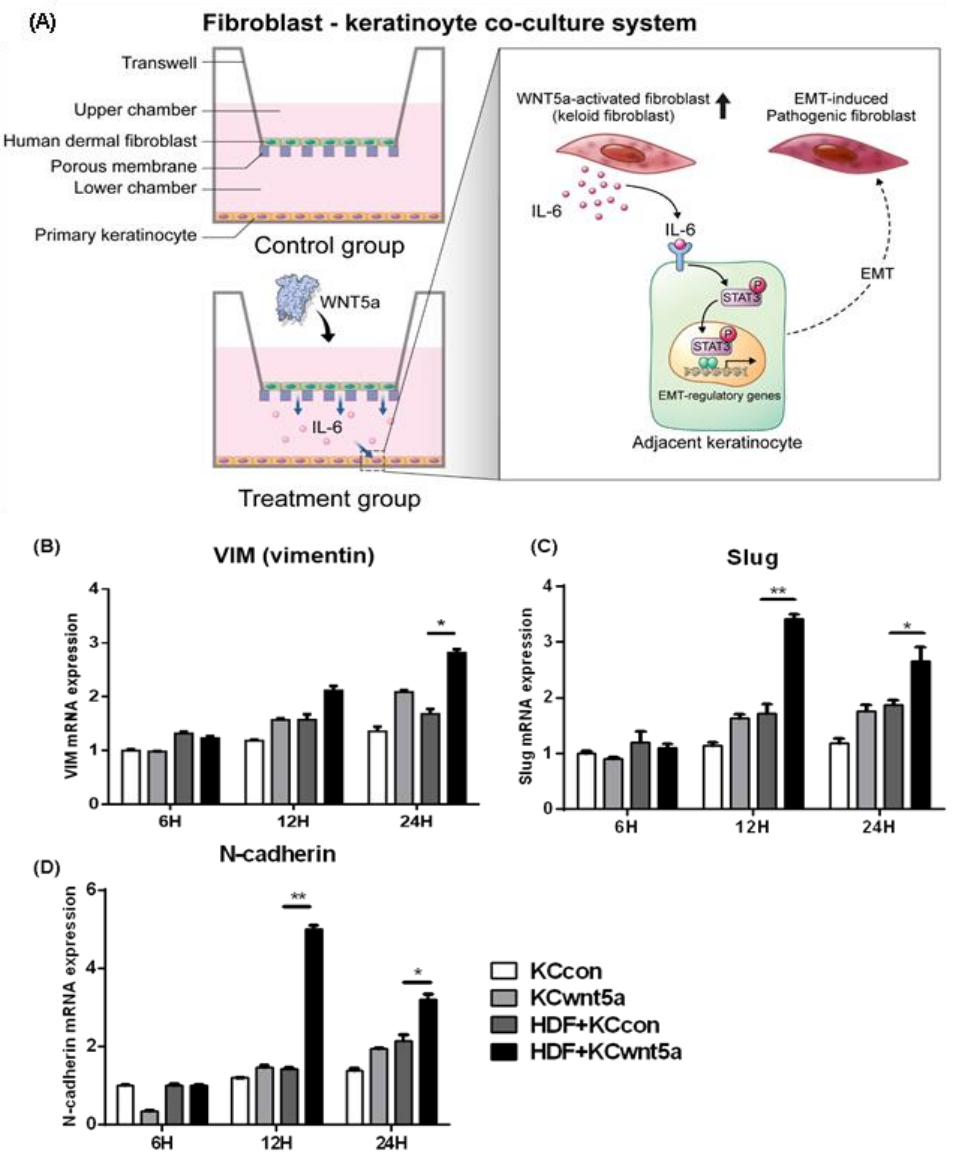

Figure 13. HEKs express higher levels of EMT markers when treated with WNT5A-treated HDFs. The animated view for the established co-culture system between HEKs and HDFs (A). The increased expressions of vimentin (B), slug (C), and N-cadherin (D) from HEKs when co-treated with WNT5A-activated HDFs (*p<0.05, **p<0.01, repeated measures ANOVA).

11. Treatment with WNT5A on HDFs produces increased secretion of IL-6

To identify the chemical mediators secreted from WNT5A-activated HDFs that may have caused EMT in co-cultured HEKs, we measured IL-6 release from HDFs activated by WNT5A. The previously performed human cytokine array revealed that KFs, which were hypothesized to have aberrantly activated WNT5A signal, secreated elevated levels of pro-inflammatory cytokines, including IL-6. Hence, HDFs (5×10^5 cells) were cultured with or without 250 ng/mL WNT5A for 6, 12, 24, and 48 h. ELISA revealed significantly increased secretion of IL-6 from fibroblasts treated with WNT5A for 24 and 48 h (Fig. 14). Thus, WNT5A aberrantly activated HDFs, and IL-6 secreted by these cells affected co-cultured HEKs and resulted in EMT.

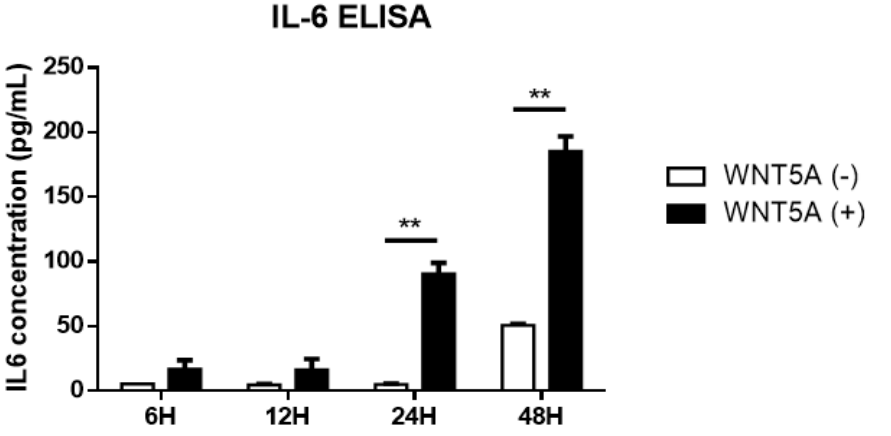

Figure 14. Increased production of pro-inflammatory IL-6 from WNT5A-treated HDFs (p<0.01).**

12. Conditioning with IL-6 causes EMT in HEKs

The previous sections of our study showed that WNT5A-activated HDFs produces significantly higher level of IL-6. Moreover, co-culturing HEKs with WNT5A-activated HDFs allowed increased expression of EMT markers from HEKs. To evaluate the role of IL-6 in EMT, we seeded HEKs into plates cultured the cells with or without 50 ng/mL recombinant IL-6 for 6 and 24 h. IL-6-treated HEKs showed significant reduction of E-cadherin after 6 and 24 h (Fig. 15A, $*p < 0.05$, $***p < 0.005$). In contrast, gene expression of N-cadherin and vimentin was significantly increased at 24 h after treatment with IL-6 (Fig. 15B-C, $***p < 0.005$).

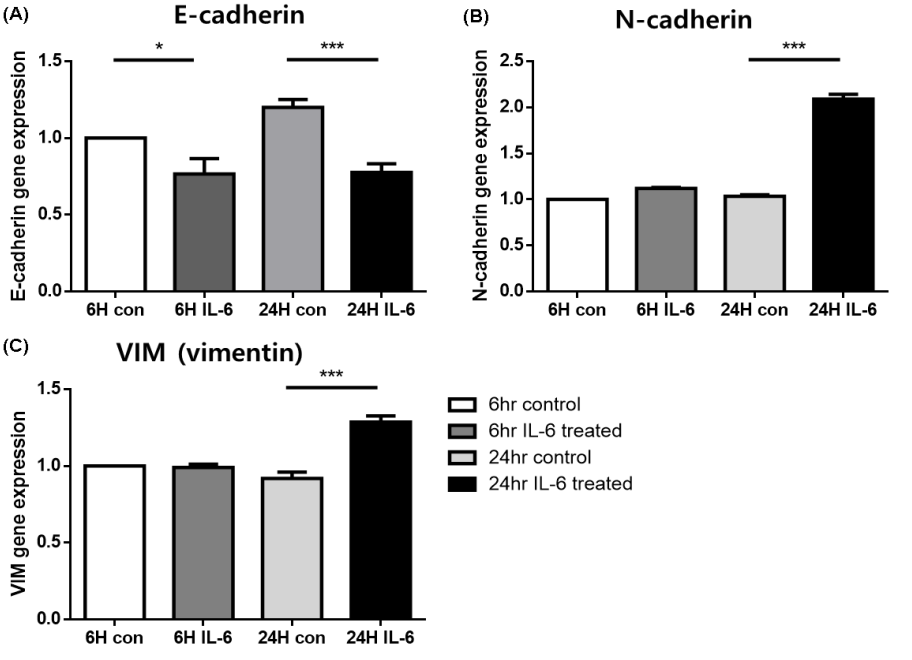

Figure 15. mRNA expression levels of EMT markers for HEKs cultured with or without IL-6. Expression of E-cadherin (A), N-cadherin (B), and vimentin (C) as the EMT markers after treatment with recombinant IL-6 for 6h and 24h.

13. IL-6 produced by WNT5A-stimulated fibroblasts cause increased EMT on co-cultured keratinocytes via JAK/STAT pathway

Western blot analysis revealed increased levels of vimentin and Slug in HEKs co-treated with WNT5A for 24 h. E-cadherin showed decreased expression in HEKs co-cultured with WNT5A-activated fibroblasts. Phosphorylated-STAT (*p*-STAT) expression was higher in HEKs co-cultured with WNT5A-activated fibroblasts compared to with WNT5A-untreated keratinocytes. Interestingly, keratinocytes did not express *p*-STAT with or without stimulation with WNT5A when they were cultured without fibroblasts (Fig. 16A-E).We next directly treated keratinocytes with 50 ng/mL recombinant IL-6 to observe its effect on JAK/STAT pathway activation and subsequent EMT (Fig. 16F). IL-6 induced increased expression of *p*-STAT, N-cadherin, and Slug, whereas the expression of E-cadherin was decreased. Therefore, IL-6 secreted from WNT5A-activated fibroblasts caused EMT in adjacent keratinocytes.

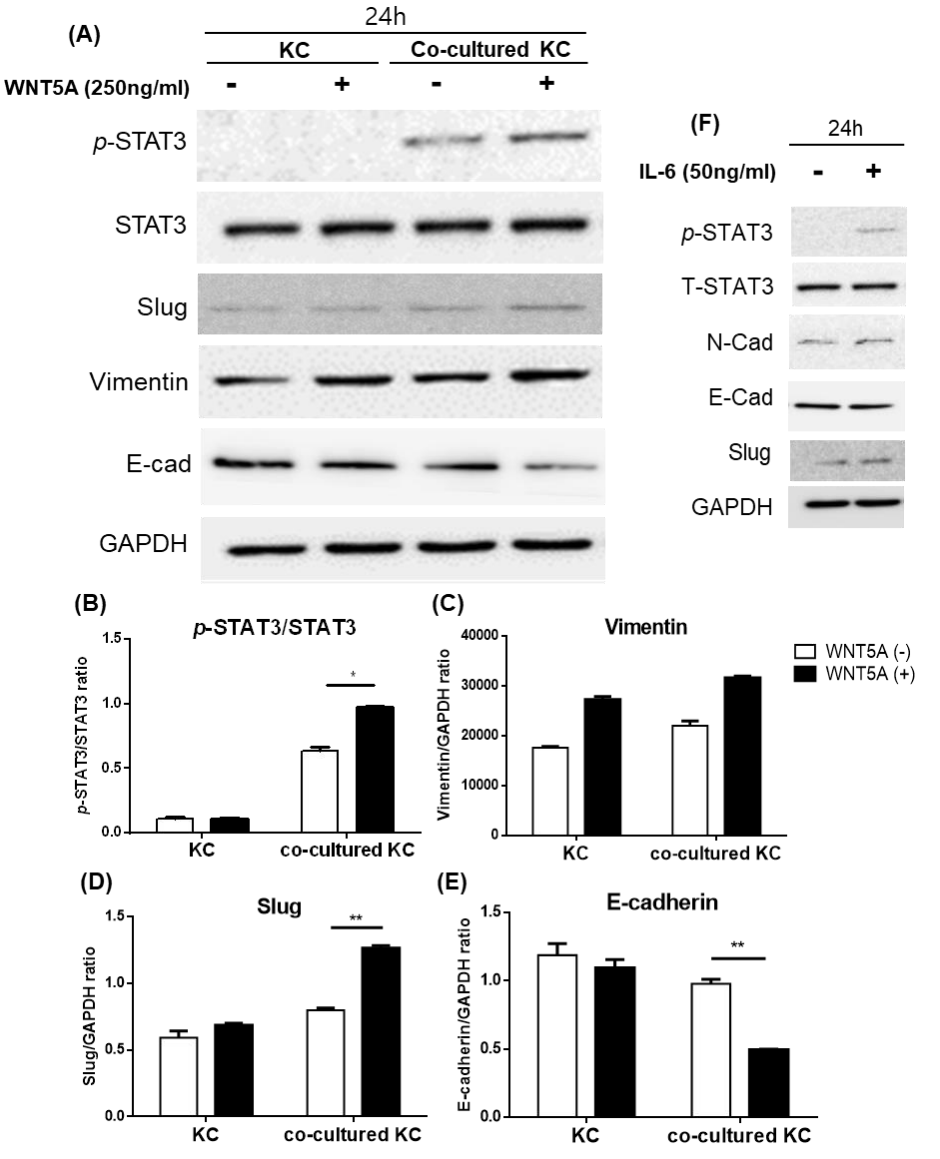

Figure 16. Western blot analysis of keratinocytes cultured with or without human dermal fibroblasts (A). Expression of *p*-STAT/STAT (B), vimentin (C), slug (D) as the EMT markers, and E-cadherin (E) after treatment with WNT5A for 24h. Western blot analysis of keratinocytes cultured with or without treatment with IL-6 (F).

14. WNT5A knockdown decreased the production of IL-6 from fibroblasts and increased the expression of EMT markers on co-cultured keratinocytes

RNA silencing of WNT5A (siWNT5A) was performed to confirmed its role in the production of IL-6 and subsequent elevation of EMT markers from adjacent keratinocytes. Whereas HDFs after transfection of cells with siWNT5A did not differ in the level of IL-6 production, KFs showed significant reduction of the production of IL-6 when transfected with siWNT5A (Fig. 17A).

We next performed qRT-PCR on HEKs co-cultured with HDFs and KFs which underwent RNA silencing of WNT5A (HEK+KFsiWNT5A). It revealed that HEKs co-cultured with KFs treated with siWNT5A for 48h expressed significantly reduced levels of EMT markers, a-SMA, N-cadherin, vimentin compared to HEKs which were co-cultured with KFs treated with control siRNA (HEK+KFsiCont, Fig 17B-D).

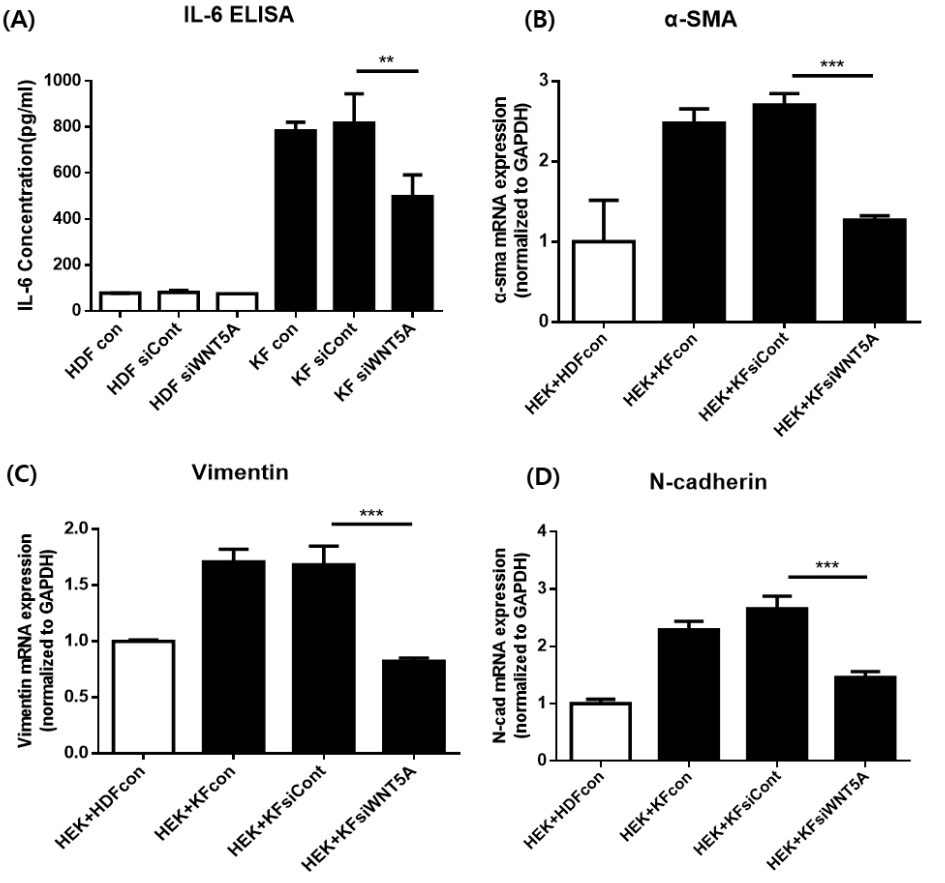

Figure 17. The effect of RNA silencing of WNT5A on the production of IL-6 and the expressions of EMT markers. (A) Production of IL-6 from HDF control, HDFs treated with control siRNA, HDFs treated with siWNT5A, KFs control, KFs treated with control siRNA, and KFs treated with siWNT5A. mRNA expression levels of (A) α-SMA, (B) vimentin, (C) N-cadherin on HEKs co-cultured with HDFs, KFs, KFs treated with control siRNA, and KFs treated with siWNT5A.

IV. DISCUSSION

Although much has been discovered on keloid pathogenesis over the past several decades, the current understanding of its molecular drivers still remains incomplete. In various fibrotic diseases such as keloids, certain disease-specific triggers initiate local site inflammation, which can activate a distinct cell population that drives fibrosis in susceptible individuals [20]. Shared central fibrotic signaling pathways such as TGF-β, PDGF, Wnt, and hedgehog signaling, lead to disease progression in fibrotic diseases that include keloid scars as well as highly prevalent chronic diseases such as asthma, chronic obstructive pulmonary disease, atherosclerosis, and inflammatory bowel diseases [20]. In this study, we analyzed DEG by next-generation RNA sequencing of keloid and normal tissues to identify genes contributing to keloid formation and aggravation. Notably, Gene Set Enrichment Analysis of the DEGs revealed that upregulated genes in keloid tissues were most highly enriched in the pathway of EMT gene signatures. Additionally, representative gene sets related to EMT, including VIM, SNAI, CDH2, and ACTA2, were simultaneously upregulated in keloid tissues. Increased expression of EMT markers was observed in keloid tissues compared to in normal tissues.

Few high-quality translational studies have focused on keloids, particularly because of the lack of a validated animal model. Keloids only occur in humans, making it difficult to study the pathogenesis of the disease [21]. As spontaneous keloid scar formation in an animal model is not possible, currently available keloid animal models involve keloid reproduction either by inducing abnormal fibrosis or implantation of human keloid tissues [22]. We generated an *in vivo* keloid animal model by using bleomycin-induced skin fibrosis in C57/BL6 mice as described in previous studies for tissue fibrosis such as systemic sclerosis and cutaneous graft-versus-host disease [23]. Bleomycin triggers the production of ROS,

which can damage the surrounding cells, leading to the recruitment of inflammatory cells and aberrant activation of resident fibroblasts [24]. Our fibrosis model showed significantly increased expression of EMT markers such as vimentin as well as WNT5A, which is consistent with the human tissue immunohistochemistry and laboratory test results, indicating the successful reproduction of keloid scars via bleomycin-intradermal injection in mice and potential role for WNT5A in keloid pathogenesis and EMT.

The current study uncovered a rather strong WNT5A transcription that was upregulated in keloid tissues. WNT5A activates non-canonical Wnt pathways, and its overexpression has been observed in the progression of tumorigenesis by promoting cell motility, EMT, and metastasis [25]. The correlation of WNT5A with increased EMT was previously detected in various studies of cancer development [26-28]. Increasing evidence has also indicated a central role for Wnt signaling in driving fibrotic responses, including liver, kidney, and lung fibrosis [29-31]. Previous studies pointed to a connection between WNT5A and the fibrogenic factor TGF-β, necessitating further studies of the functional role of WNT5A in fibrotic diseases [15,28,32]. We found that the expression of WNT5A, EMT markers, and IL-6/JAK/STAT3 pathway was notably upregulated in keloid scars. Thus, WNT5A and the JAK/STAT3 pathway may play an essential role in various types of neoplasms and in the pathogenesis of keloid development [33].

The role of WNT5A in the tumor microenvironment by stimulating the production of various pro-inflammatory cytokines that drive tumor invasion has recently gained attention in cancer research. Cytokines most commonly known to be upregulated by WNT5A include IL-1, CXCL8 (IL-8), CCL2 (MCP-1), and IL-6 [25]. Among them, IL-6 overexpression by tumor-associated fibroblasts was reported in invasive tumors such as melanoma [34,35]. Interestingly, we observed increased expression of MCP-1, CXCL1, IL-8, and IL-6 in media cultured with

keloid fibroblasts compared to in that cultured with HDFs. Additionally, keloid fibroblasts expressed higher levels of WNT5A compared to HDFs. Our results also suggested that WNT5A-activated fibroblasts secrete higher levels of IL-6, thus affecting adjacent keratinocytes to express invasive properties as shown in keloids.

IL-6 and one of its numerous downstream mediators, JAK/STAT3 pathway, are aberrantly hyperactivated in many types of cancers, thus driving tumor cell proliferation, invasiveness, and EMT [36,37]. Geo et al. (2017) demonstrated that IL-6 induced EMT through the JAK/STAT3 pathway in hepatocellular carcinoma, which in turn accelerated cancer invasiveness. We observed activation of the IL-6/JAK/STAT3 pathway in co-cultured fibroblasts treated with WNT5A and subsequent elevation of EMT markers in keratinocytes[38]. The WNT5A knockdown via tranfection of keloid fibroblasts with siWNT5A decreased the production IL-6 and increased the expression of EMT markers on adjacent keratinocytes. These results indicate an indirect role for WNT5A via fibroblasts, which produces increased level of IL-6, on adjacent keratinocytes to undergo EMT.

To our knowledge, this is the first description of the use of next generation RNA sequencing in primary human keloid tissue to describe its pathogenesis. As the medical need for effective anti-fibrotic therapies is very high, understanding pathogenesis of keloid and developing targeted therapies is necessary. Our study reveals the novel responsible gene in keloid pathogenesis, WNT5A, which drives aberrant activation of dermal fibroblasts and subsequent process of EMT in adjacent keratinocytes via IL-6/JAK/STAT3 pathway. Further experiments are needed to evaluate its potential role as a keloid biomarker and to develop new treatment targets in keloid and skin fibrosis research.

V. CONCLUSION

WNT5A has a potential role as novel keloid biomarker. It is significantly elevated in human keloid tissues and fibrosis-induced animal model compared to normal skin. WNT5A indirectly affects EMT by hyperactivating regional fibroblasts to produce pro-inflammatory cytokine, IL-6, to adjacent keratinocytes to undergo JAK/STAT3 pathway-medicated EMT. Further studies are needed on WNT5A to develop new diagnostic and treatment modalities in keloid and fibrosis research.

REFERENCES

1. Wesseling M, Sakkers TR, de Jager SCA, Pasterkamp G, Goumans MJ. The morphological and molecular mechanisms of epithelial/endothelial-to-mesenchymal transition and its involvement in atherosclerosis. Vascul Pharmacol 2018;106:1-8.
2. Kang Y, Roh MR, Rajadurai S, Rajadurai A, Kumar R, Njauw CN, et al. Hypoxia and HIF-1alpha Regulate Collagen Production in Keloids. J Invest Dermatol 2020.
3. Tan S, Khumalo N, Bayat A. Understanding Keloid Pathobiology From a Quasi-Neoplastic Perspective: Less of a Scar and More of a Chronic Inflammatory Disease With Cancer-Like Tendencies. Front Immunol 2019;10:1810.
4. Dongre A, Weinberg RA. New insights into the mechanisms of epithelial-mesenchymal transition and implications for cancer. Nat Rev Mol Cell Biol 2019;20:69-84.
5. Kalluri R, Weinberg RA. The basics of epithelial-mesenchymal transition. J Clin Invest 2009;119:1420-8.
6. Lamouille S, Xu J, Derynck R. Molecular mechanisms of epithelial-mesenchymal transition. Nat Rev Mol Cell Biol 2014;15:178-96.
7. Nakamura M, Tokura Y. Epithelial-mesenchymal transition in the skin. J Dermatol Sci 2011;61:7-13.
8. Kuwahara H, Tosa M, Egawa S, Murakami M, Mohammad G, Ogawa R. Examination of Epithelial Mesenchymal Transition in Keloid Tissues and Possibility of Keloid Therapy Target. Plast Reconstr Surg Glob Open 2016;4:e1138.
9. Bussard KM, Mutkus L, Stumpf K, Gomez-Manzano C, Marini FC. Tumor-associated stromal cells as key contributors to the tumor microenvironment. Breast Cancer Res 2016;18:84.
10. Lim CP, Phan TT, Lim IJ, Cao X. Stat3 contributes to keloid pathogenesis via promoting collagen production, cell proliferation and migration. Oncogene 2006;25:5416-25.

11. Chang Q, Bournazou E, Sansone P, Berishaj M, Gao SP, Daly L, et al. The IL-6/JAK/Stat3 feed-forward loop drives tumorigenesis and metastasis. Neoplasia 2013;15:848-62.
12. Xiao J, Gong Y, Chen Y, Yu D, Wang X, Zhang X, et al. IL-6 promotes epithelial-to-mesenchymal transition of human peritoneal mesothelial cells possibly through the JAK2/STAT3 signaling pathway. Am J Physiol Renal Physiol 2017;313:F310-F8.
13. Dong S, Wu C, Hu J, Wang Q, Chen S, Wang Z, et al. Wnt5a Promotes Cytokines Production and Cell Proliferation in Human Hepatic Stellate Cells Independent of Canonical Wnt Pathway. Clin Lab 2015;61:537-47.
14. Rashid ST, Humphries JD, Byron A, Dhar A, Askari JA, Selley JN, et al. Proteomic analysis of extracellular matrix from the hepatic stellate cell line LX-2 identifies CYR61 and Wnt-5a as novel constituents of fibrotic liver. J Proteome Res 2012;11:4052-64.
15. Beljaars L, Daliri S, Dijkhuizen C, Poelstra K, Gosens R. WNT-5A regulates TGF-beta-related activities in liver fibrosis. Am J Physiol Gastrointest Liver Physiol 2017;312:G219-G27.
16. Fei T, Yu T. scBatch: batch-effect correction of RNA-seq data through sample distance matrix adjustment. Bioinformatics 2020;36:3115-23.
17. Tirosh I, Izar B, Prakadan SM, Wadsworth MH, 2nd, Treacy D, Trombetta JJ, et al. Dissecting the multicellular ecosystem of metastatic melanoma by single-cell RNA-seq. Science 2016;352:189-96.
18. Sekiguchi A, Motegi SI, Fujiwara C, Yamazaki S, Inoue Y, Uchiyama A, et al. Inhibitory effect of kaempferol on skin fibrosis in systemic sclerosis by the suppression of oxidative stress. J Dermatol Sci 2019;96:8-17.
19. Loh CY, Chai JY, Tang TF, Wong WF, Sethi G, Shanmugam MK, et al. The E-Cadherin and N-Cadherin Switch in Epithelial-to-Mesenchymal Transition: Signaling, Therapeutic Implications, and Challenges. Cells 2019;8.
20. Distler JHW, Gyorfi AH, Ramanujam M, Whitfield ML, Konigshoff M, Lafyatis R. Shared and distinct mechanisms of fibrosis. Nat Rev Rheumatol

2019;15:705-30.

21. Sharma JR, Lebeko M, Kidzeru EB, Khumalo NP, Bayat A. In Vitro and Ex Vivo Models for Functional Testing of Therapeutic Anti-scarring Drug Targets in Keloids. Adv Wound Care (New Rochelle) 2019;8:655-70.
22. Limandjaja GC, Niessen FB, Scheper RJ, Gibbs S. The Keloid Disorder: Heterogeneity, Histopathology, Mechanisms and Models. Front Cell Dev Biol 2020;8:360.
23. Do NN, Eming SA. Skin fibrosis: Models and mechanisms. Curr Res Transl Med 2016;64:185-93.
24. Batteux F, Kavian N, Servettaz A. New insights on chemically induced animal models of systemic sclerosis. Curr Opin Rheumatol 2011;23:511-8.
25. Lopez-Bergami P, Barbero G. The emerging role of Wnt5a in the promotion of a pro-inflammatory and immunosuppressive tumor microenvironment. Cancer Metastasis Rev 2020;39:933-52.
26. Wang B, Tang Z, Gong H, Zhu L, Liu X. Wnt5a promotes epithelial-to-mesenchymal transition and metastasis in non-small-cell lung cancer. Biosci Rep 2017;37.
27. Qi H, Sun B, Zhao X, Du J, Gu Q, Liu Y, et al. Wnt5a promotes vasculogenic mimicry and epithelial-mesenchymal transition via protein kinase Calpha in epithelial ovarian cancer. Oncol Rep 2014;32:771-9.
28. Kumawat K, Menzen MH, Bos IS, Baarsma HA, Borger P, Roth M, et al. Noncanonical WNT-5A signaling regulates TGF-beta-induced extracellular matrix production by airway smooth muscle cells. FASEB J 2013;27:1631-43.
29. Jiang F, Parsons CJ, Stefanovic B. Gene expression profile of quiescent and activated rat hepatic stellate cells implicates Wnt signaling pathway in activation. J Hepatol 2006;45:401-9.
30. Li X, Yamagata K, Nishita M, Endo M, Arfian N, Rikitake Y, et al. Activation of Wnt5a-Ror2 signaling associated with epithelial-to-mesenchymal transition of tubular epithelial cells during renal fibrosis. Genes Cells 2013;18:608-19.

31. Vuga LJ, Ben-Yehudah A, Kovkarova-Naumovski E, Oriss T, Gibson KF, Feghali-Bostwick C, et al. WNT5A is a regulator of fibroblast proliferation and resistance to apoptosis. Am J Respir Cell Mol Biol 2009;41:583-9.
32. Kumawat K, Menzen MH, Slegtenhorst RM, Halayko AJ, Schmidt M, Gosens R. TGF-beta-activated kinase 1 (TAK1) signaling regulates TGF-beta-induced WNT-5A expression in airway smooth muscle cells via Sp1 and beta-catenin. PLoS One 2014;9:e94801.
33. Jin W. Role of JAK/STAT3 Signaling in the Regulation of Metastasis, the Transition of Cancer Stem Cells, and Chemoresistance of Cancer by Epithelial-Mesenchymal Transition. Cells 2020;9.
34. Tsukamoto H, Fujieda K, Hirayama M, Ikeda T, Yuno A, Matsumura K, et al. Soluble IL6R Expressed by Myeloid Cells Reduces Tumor-Specific Th1 Differentiation and Drives Tumor Progression. Cancer Res 2017;77:2279-91.
35. Hoejberg L, Bastholt L, Schmidt H. Interleukin-6 and melanoma. Melanoma Res 2012;22:327-33.
36. Johnson DE, O'Keefe RA, Grandis JR. Targeting the IL-6/JAK/STAT3 signalling axis in cancer. Nat Rev Clin Oncol 2018;15:234-48.
37. Sullivan NJ, Sasser AK, Axel AE, Vesuna F, Raman V, Ramirez N, et al. Interleukin-6 induces an epithelial-mesenchymal transition phenotype in human breast cancer cells. Oncogene 2009;28:2940-7.
38. Gao Y, Li W, Liu R, Guo Q, Li J, Bao Y, et al. Norcantharidin inhibits IL-6-induced epithelial mesenchymal transition via the JAK2/STAT3/TWIST signaling pathway in hepatocellular carcinoma cells. Oncol Rep 2017;38: 1224-32.

ABSTRACT (IN KOREAN)

켈로이드 병인 내 IL-6/JAK/STAT3 세포신호전달체계를 통한 WNT5A 매개 상피-중간엽 전이 경로 탐색

<지도교수 이주희>

연세대학교 대학원 의학과

이 영 인

켈로이드는 수술이나 외상 혹은 피부의 염증성 질환으로 인한 손상이 있은 뒤 회복하는 과정에서 섬유아세포 (fibroblast)의 과도한 활성화로 인해 세포 외 기질의 주요 구성성분인 콜라겐이 과다하게 침착 되어 발생하는 질환이다. 켈로이드는 붉고 단단하며 심한 가려움증이나 통증을 동반할 수 있으며 발생 부위에 따라 움직임 장애를 동반하는 경우도 있다. 의학 기술의 개발로 다양한 수술, 레이저, 도포약제 등 다양한 치료제들이 개발되었지만 대부분 방법들이 재발율이 매우 높아 만성 난치성 질환으로 분류된다.

병인성 섬유아세포 (pathogenic fibroblast)는 정상 섬유아세포와 비교하며 분화 및 증식이 항진되어 있으며, 악성종양 조직에서 주로 나타나는 epithelial-to-mesenchymal transition과 관련된 표현형을 보이는 것으로 보고되고 있다. 또한 켈로이드에서 유래한 섬유모세모

(fibroblast) 배양 시 근섬유화세포 (myofibroblast)와 같은 표현형을 보인다는 특징이 있다. 병인성 섬유아세포의 기능에 영향을 주는 대표적인 인자들로 물리적 장력, 조직 내 저산소분압 그리고 과도한 염증반응을 들 수 있다. 켈로이드 흉터에서 피부 섬유화의 주된 역할을 하는 병인성 섬유화세포의 기원은 아직 논쟁이 되고 있으나 특발성 폐 섬유증을 포함한 타 장기의 만성 진행성 섬유화 질환 모델에서 악성종양에서 보이는 epithelial-to-mesenchymal transition을 통한 근섬유아세포의 형성이 보고된 바 있다. 최근에는 방사선에 의한 조직 섬유화 과정 중 혈관내피세포 (endothelial cell)가 endothelial-to-mesenchymal transition을 통해 병인성 섬유화세포의 기원 중 하나로 규명되고 있다. 이 밖에도 켈로이드를 포함한 피부 섬유화 질환의 경우 주변의 풍부한 resident fibroblast가 물리적 장력 및 과도한 염증성 싸이토카인의 분비로 인하여 근섬유화세포와 같은 표현형을 보인다 라는 주장이 제기되고 있으나 직접적인 조절기전은 정확히 규명되고 있지 않다.

본 연구에서는 켈로이드의 발병에 기여하는 원인 유전자를 규명하기 위하여 정상 조직과 켈로이드 조직에서 차세대 유전체 분석기술인 RNA 염기서열분석을 이용하여 두 군간 전사체 발현 정도의 차이를 확인하였다. 분석된 켈로이드 전사체의 발현 정도를 생물정보학적 분석기술을 이용하여 발굴한 WNT5A의 활성화를 질환의 예후를 예측하는 바이오마커이자 새로운 치료의 타겟으로 제시하고자 한다.

핵심되는 말: 창상치유, 켈로이드, 비후성 흉터, 피부섬유화